E951 Targetry Neutron Studies

Al Zeller, Reg Ronningen – NSCL/MSU

Lawrence Heilbronn – LBNL

Paul Goldhagen – DOE-EML

Marty Zucker – BNL

Purpose:

Measure high energy neutron spectra under different target geometries to benchmark Monte Carlo codes

Methods:

- Activation foils
- Bonner Spheres
- Time-of-flight
- ^{3}He detectors

Some activation foil measurements made for neutron energies up to 70 MeV

Measurements possible to >600 Mev with ^{197}Au, Cu and Bi(fission) foils

Unfold to give spectra

Use high intensity beam as a parasite

TANADA

Table 2 List of the reactions and associated decay data [a)]

Reaction			Q-value (MeV)	Threshold Energy (MeV)	Half-life	γ-ray Energy (keV)	γ-ray emission rate (%)
^{115}In	(n,n')	^{115m}In	-0.34	0.34	4.486 h	336.24	45.9(23)[d)]
^{93}Nb	(n,2n)	^{92m}Nb	-8.97	9.06	10.15 d	934.46	99.07(4)
	(n,4n)	^{90}Nb	-28.76	29.08	14.60 h	1129.00	92.7(5)
^{27}Al	(n,x)	^{24}Na	-3.13 [b)]	3.25	14.959 h	1368.6	100
^{209}Bi	(n,4n)	^{206}Bi	-22.45	22.56	6.243 d	803.1	98.9(1)
	(n,5n)	^{205}Bi	-29.48	29.63	15.31 d	703.4	31.1(1)
	(n,6n)	^{204}Bi	-37.90	38.08	11.22 h	984.02	58.8(4)
	(n,7n)	^{203}Bi	-45.12	45.34	11.76 h	820.3	29.6(15)
	(n,8n)	^{202}Bi	-53.97	54.24	1.72 h	960.67	99.28(2)
	(n,9n)	^{201m}Bi [c)]	-62.21	62.52	59.1 m	846.5	5.2
		^{201g}Bi	-61.63	61.67	108 m	629.1	24(5)
	(n,10n)	^{200m}Bi	-70.71	71.07	31 m	1026.5	91(7)
		^{200g}Bi	-70.51	70.51	36.4 m	1026.5	100
^{59}Co	(n,γ)	^{60}Co	5.07	0.0	5.2714 y	1173.2	99.9736(7)
	(n,p)	^{59}Fe	-0.78	0.80	44.503 d	1099.3	56.5(15)
	(n,x)	^{56}Mn	0.33	0.0	2.5785 h	845.8	98.9(3)
	(n,2n)	^{58}Co	-10.45	10.63	70.82 d	810.8	99.4
	(n,3n)	^{57}Co	-19.03	19.36	271.79 d	122.1	85.6(2)
	(n,4n)	^{56}Co	-30.40	30.95	77.27 d	846.8	99.940(25)
	(n,5n)	^{55}Co	-40.49	41.22	17.53 h	931.3	75(4)
^{169}Tm	(n,2n)	^{168}Tm	-8.03	8.08	93.1 d	198.2	52.4(16)
	(n,3n)	^{167}Tm	-14.90	14.99	9.25 d	207.8	41(8)
	(n,4n)	^{166}Tm	-23.61	23.75	7.70 h	778.8	18.9(11)
	(n,5n)	^{165}Tm	-30.63	30.31	30.36 h	242.9	35.5(17)

a) Taken from Table of Isotopes, 8th Edition.

b) for the ^{27}Al(n,α)^{24}Na reaction.

c) The branching ratios to EC(β$^+$)-decay are unknown.

d) The uncertainty of the last numerical values is shown in the parentheses.

Table 2. List of the reactions and associated decay data [a] (continued).

Reaction	Q-value (MeV)	Threshold Energy (MeV)	Half-life	γ-ray Energy (keV)	γ-ray emission rate (%)
^{89}Y (n,2n)^{88}Y	-11.48	11.61	106.65 d	898.0	93.7(3)
(n,3n)$^{87m+g}$Y	-20.83	21.07	79.8 h	388.5	82.1(5)
(n,4n)$^{86m+g}$Y	-32.86	33.24	14.74 h	1076.6	82.5(4)
(n,5n)^{85g}Y	-42.17	42.66	2.68 h	231.7	84(8)
^{nat}Ni (n,x) ^{58}Co	0.40 [b]	0.0	70.82 d	810.8	99.4
(n,x) ^{57}Co	-8.17 [c]	8.31	271.79 d	122.1	85.6(2)
^{nat}Ti (n,x) ^{48}Sc	-3.21 [d]	3.28	43.67 h	983.5	100(6)
(n,x) ^{47}Sc	-11.45 [e]	11.68	3.3492 d	159.4	68.3(4)
(n,x) ^{46g}Sc	-22.09 [f]	22.55	83.79 d	889.3	100
(n,x) ^{44m}Sc	-42.45 [g]	43.33	58.6 d	271.1	86.7
^{44g}Sc	-42.17 [h]	43.05	3.927 h	1157.0	99.9

a) Taken from Table of Isotopes, 8th Edition.

b) for the ^{58}Ni(n,p)^{58}Co reaction.

c) for the ^{58}Ni(n,np)^{57}Co reaction.

d) for the ^{48}Ti(n,p)^{48}Sc reaction.

e) for the ^{48}Ti(n,np)^{47}Sc reaction.

f) for the ^{48}Ti(n,2np)^{46g}Sc reaction.

g) for the ^{48}Ti(n,4np)^{44m}Sc reaction.

h) for the ^{48}Ti(n,4np)^{44g}Sc reaction.

i) The uncertainty of the last numerical values is shown in the parentheses.

Reaction	Energy Range (MeV)	Half Life	Typical Detector Size	Cross Section-Peak (mb)	Cross Section-High Energy (mb)	Particl Detect
$^{32}S(n,p)^{32}P$	> 3	14.3 d.	4 g disk	500[a]	10[a]	β^-
$^{27}Al(n,\alpha)^{24}Na$	> 6	15 h	16 - 6600 g	11[b]	9[b]	γ
$^{27}Al(n,x)^{22}Na$	> 25	2.6 y	17 g	30[b]	10[b]	γ
^{12}C -> ^{11}C	> 20	20.4 min	13-2700 g	90[b]	30[b]	β^+, γ
^{12}C -> ^{7}Be	> 30	53 d	17 g	18[b]	10[b]	γ
^{198}Hg -> ^{149}Tb	> 600	4.1 h	up to 500 g	2[b]	1[b]	α,γ
^{197}Au -> ^{149}Tb	> 600	4.1 h	0.5 g	1.6[b]	0.7[b]	α,γ
Cu -> ^{24}Na	> 600	14.7 h	580 g	4[c]	3.9[c]	γ
Cu -> ^{52}Mn	> 70	5.7 d	580 g	5[c]	4.6[c]	γ
Cu -> ^{54}Mn	> 80	310 d	580 g	11[c]	11[c]	γ

l Thomas (Sw90)

59)

(Ba84 and Ba91).

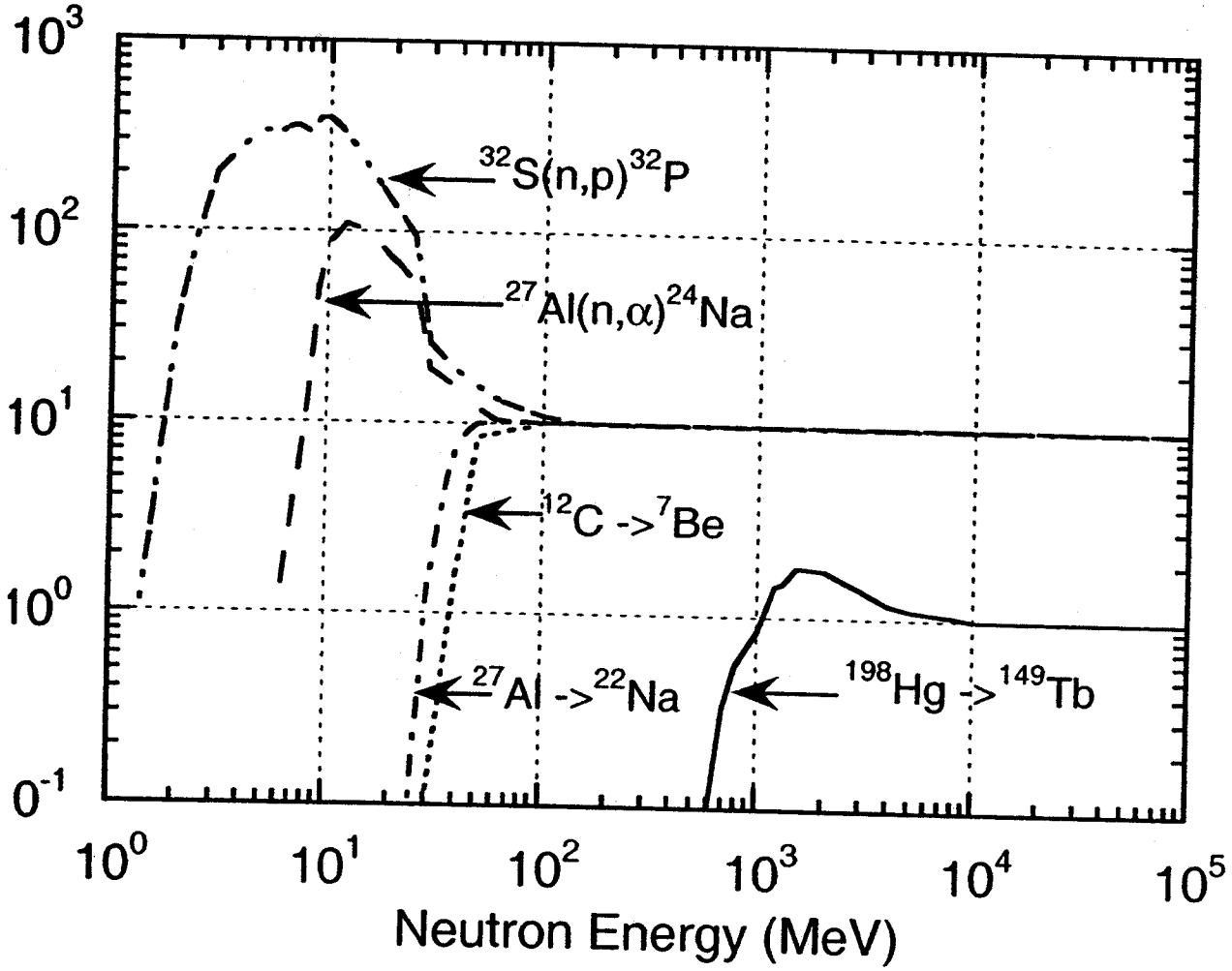

12 Excitation functions of several threshold reactions. [Adapted from (Th88).]

D. CISSART

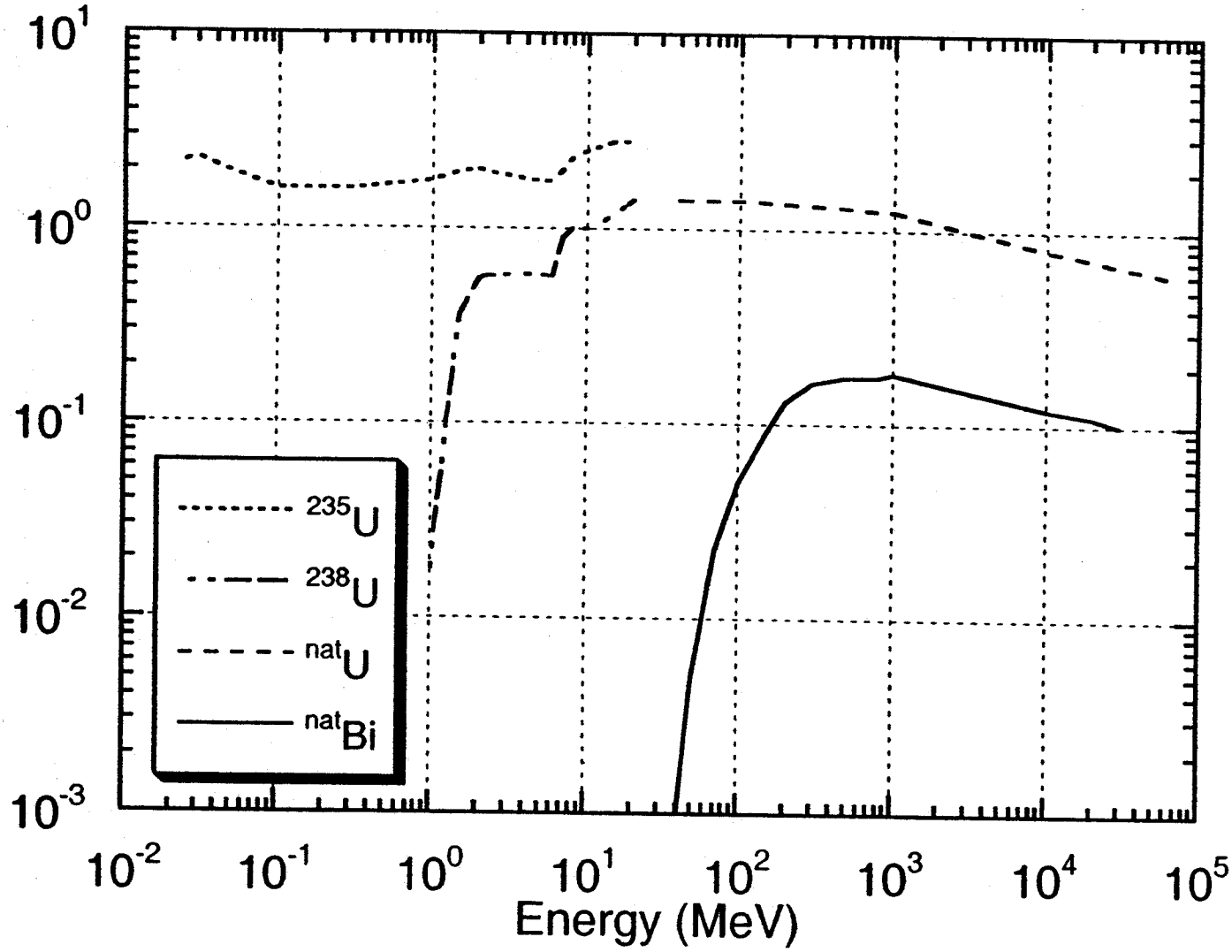

3 Fission cross sections of some common target nuclides used in fission chambers for fast neutrons. The cross sections for fission at low energies for ^{235}U are much larger. [Adaptec partially from (Kn79) and from (Sw90).]

MUSR TARGET STATION: FLUX AND DOSE

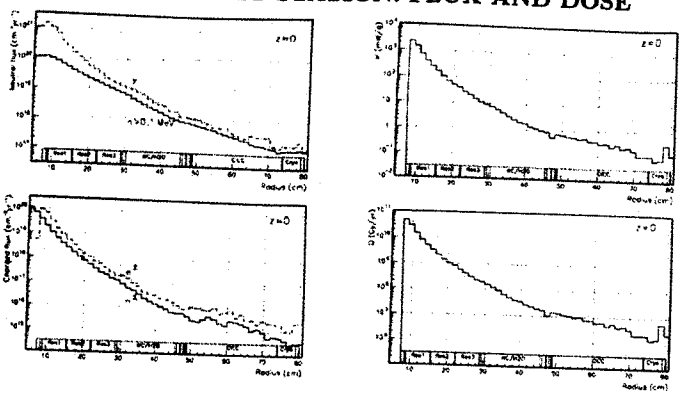

Radial distributions of particle fluxes ($cm^{-2}yr^{-1}$) (left) and power density (mW/g) and absorbed dose (Gy/yr) (right) at 1.5 MW

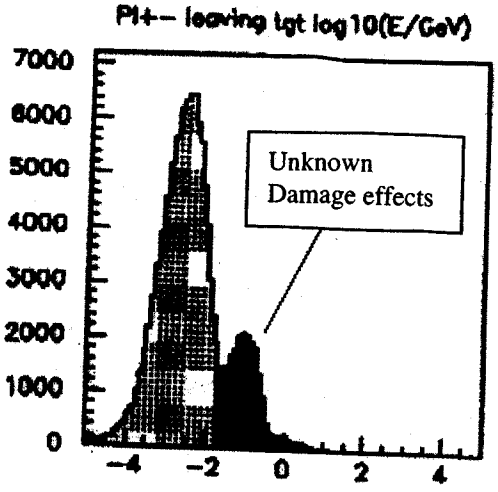

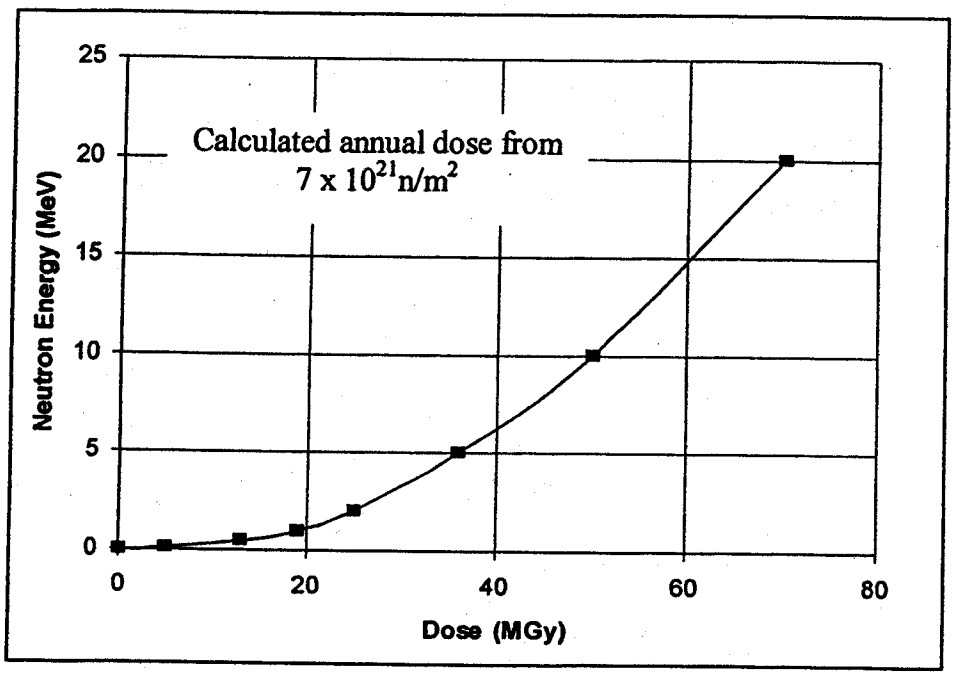

Figure 3. Fluence/dose conversion for mono-energetic neutrons (in epoxy resin).

Table 3. Assumed Neutron Energy Distribution with Calculated Dose (total neutrons: 7×10^{21} n/m^2 per year)

Fraction of Total Neutrons (%)	Energy (MeV)	Annual Dose (MGy)
[redacted] 10	[redacted] 20	[redacted] 7
[redacted] 20	[redacted] 10	[redacted] 10
20	5	7
20	1	4
20	0.5	3
10	0.1	1
Total (annual) dose		32

In epoxies:

Dose equivalent = fast neutron absorbed dose X "quality factor" + gamma dose

fast neutron "quality factor" = **10** (from energy deposition)

so

$(32X10)+10 = 3.3X10^{8}$ Gy/year

Problems with all inorganic magnets

Low overall current density
Availability of materials
Expensive
How robust?
Learning curve

Problems with non-hard magnets

They die young

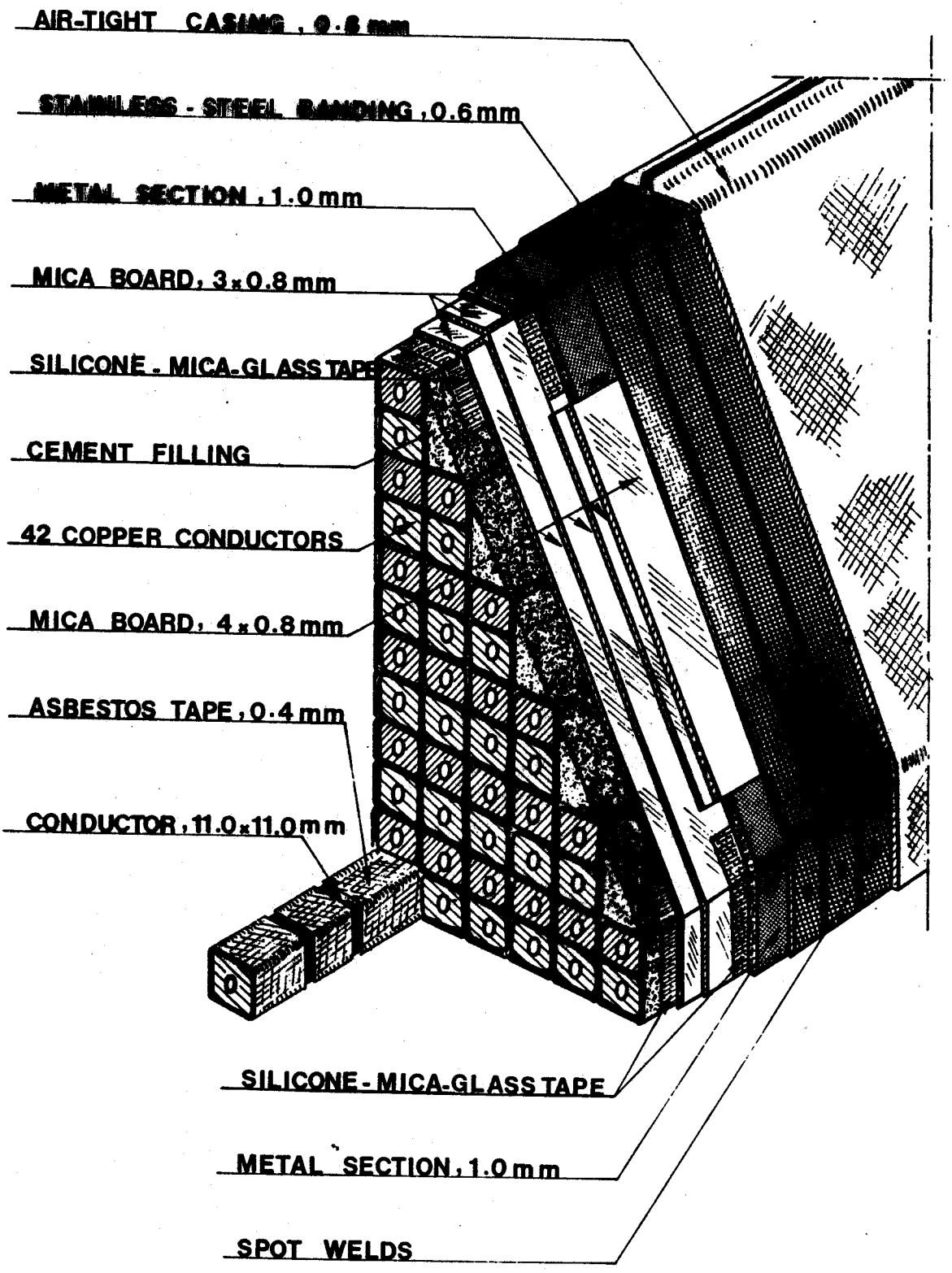

Fig. 20 QNL-B coil construction

The 0.6 to 1.0 mm wide gap is then impregnated with high-alumina cement, which adheres well to the sandblasted conductor and the asbestos tape. Other inorganic materials, such as E-glass tape, have been considered, but rejected on mechanical or chemical grounds.

The insulation is non-tracking and there is no outgassing when it is sufficiently dry, but it is rather porous. The dielectric properties of the asbestos cement may therefore be neglected, and the electrical insulation then depends on the 0.6 to 1.0 mm spacing between the conductors. This gap provides sufficient insulation, taking into account the low voltage drop between adjacent conductors, which will not exceed a few tens of volts.

nd a new idea to solve
id conductor MIC, i.e.
ls concerning the solid
section III.

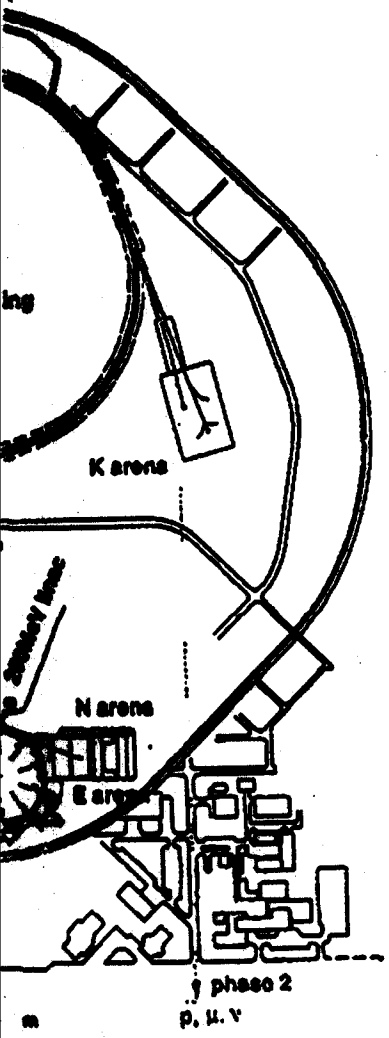

50GeV/10 μA Main Ring and
arena is an experimental area
aremas are for muons, neutrons
8GeV beam. Fast extraction
d for neutrino-beam production.
existing tunnel of the former
TRISTAN, which is now being
collider.

was wound by [illegible]
mounted on a test iron core. Many test were performed as an actual electromagnet, e.g. water-flow rates, electric resistance, and excitation function of the magnet. No serious difference was found from the design value of the coil and the magnet. Then, a long-term test of its stability and reliability with full power excitation was performed for more than one year, i.e. full-current excitation for eight hours was performed every month. The test magnet was free from any serious faults during the long-term test. The test magnet assembled with the 2500A-class MIC is shown in Photo 1. The typical operation point of

TABLE I

Dimensions and Basic Parameters of the 2500A-Class MIC

Nominal current	2500A
Outside diameter	23.8mm
Sheath thickness	1.1mm
Insulator wall thickness	1.8mm
Conductor outside diameter	18.0mm
Conductor inner diameter	10.0mm
Cross sectional area: conductor	211.7mm2
: hollow	98.6mm2
Material: Sheath	PVD,C1220(JIS)
: Conductor	OFC,C1020(JIS)

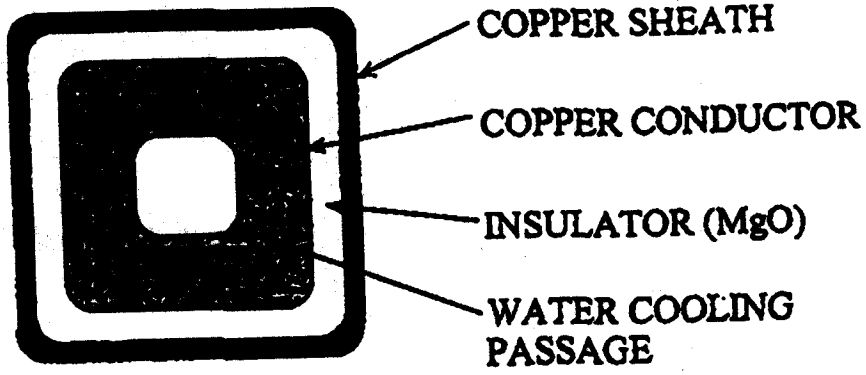

Fig. 2. Typical cross-section of the hollow conductor MIC.

avoid the corrosion problem, whatever its source, and the m.i. technique is particularly well suited to this concept, because of the relatively high thermal conductivity of the insulation (2.36 W/m•K) and the copper-jacketed construction that provides a metallic heat path to the cooling sink. This paper describes the design optimization of such a coil. The other advantages of the method may be worth mentioning: less sensitivity to the quality, (or conductivity) of the cooling water, and the absence of electrical insulators in the cooling water system.

COIL DESIGN

An application requiring radiation-hardening of the magnet coil is the beam transport line for the Fusion Materials Irradiation Test (FMIT) [9] accelerator target, where the final quadrupoles are exposed to not only the estimated 3-μA/m deuteron spill, but also to back-streaming neutrons from the target [10].

The magnet cross section chosen is shown in Fig. 1. It provides a compact structure, easily fabricated for fourfold symmetry, yet can be split readily on the horizontal centerline for remote access to the vacuum system. The coil has two layers of 13.5-mm square solid m.i. cable wound on top of a layer of cooling tubing, which therefore cools the iron parts of the magnet, removing the radiation-deposited heat.

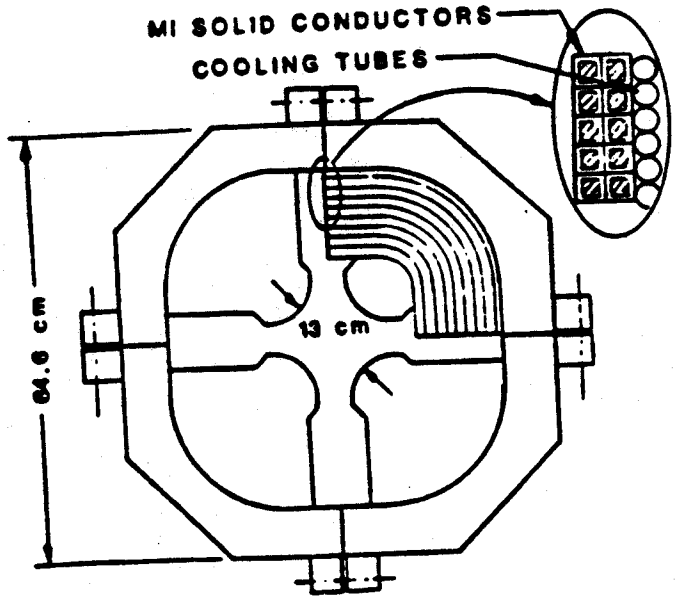

Fig. 1. Mineral-insulated, solder-potted, indirectly cooled High-Energy Beam Transport (HEBT) 30-cm quadrupole.

In Appendix 1, the heat-flow analysis of the coil is outlined, neglecting temperature-dependent terms in the electrical and thermal conductivity. For the conductor used, and the required current of 1200 A, the maximum temperature rise is less than 70 C°. For a maximum temperature of 250°C, which is recommended for copper-clad m.i. cable [11], the current can be 4300 A, giving a current density of 17.7 A/mm^2. This current density compares favorably with a directly cooled conductor, despite the 46% packing factor. A temperature map of the coil cross section is shown in Fig. 2.

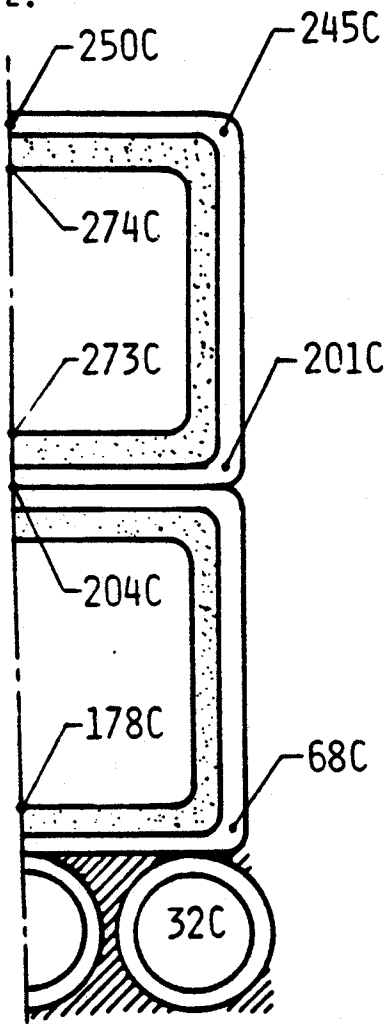

Fig. 2. Temperature map.

FUTURE DEVELOPMENT

The fusion program leads to requirements for coils of much higher current ratings than that described above [12]. Meeting these requirements calls for some changes in m.i. cable technology. Existing cables are made by minor changes in the manufacturing process for conventional m.i. cables; cables for high-power coils will require careful optimization of the cable parameters. Examination of (A-1) in the Appendix shows the following features.

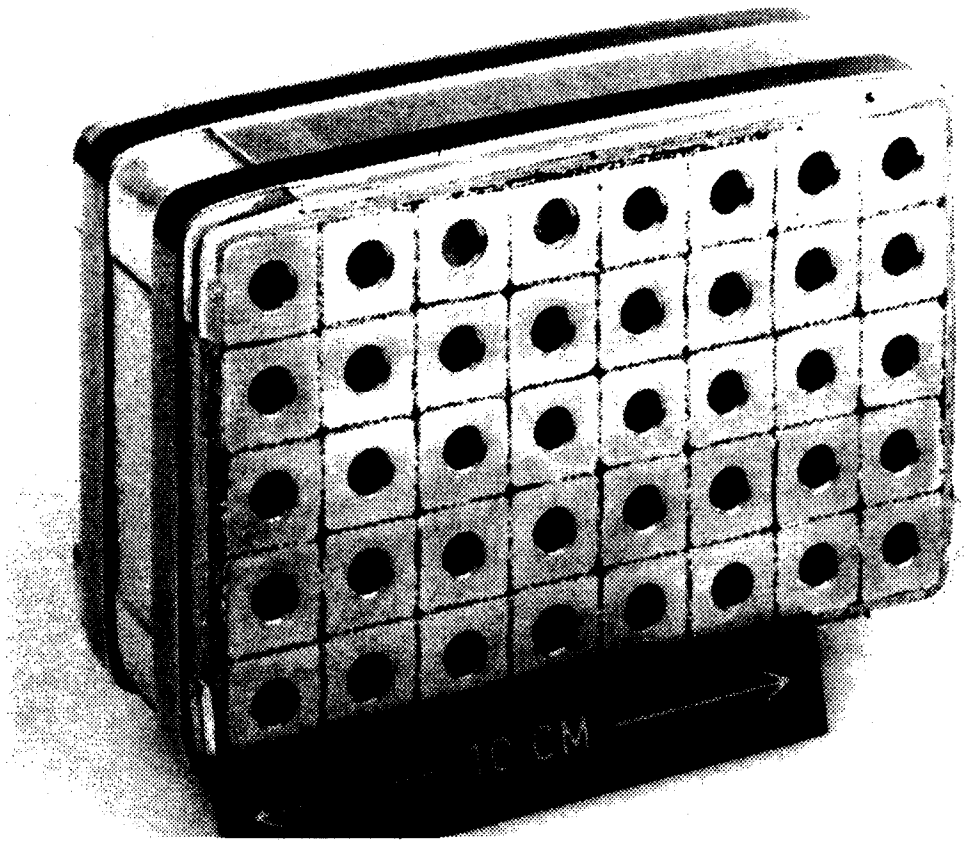

Fig. 21 The cross-section of a bending magnet coil

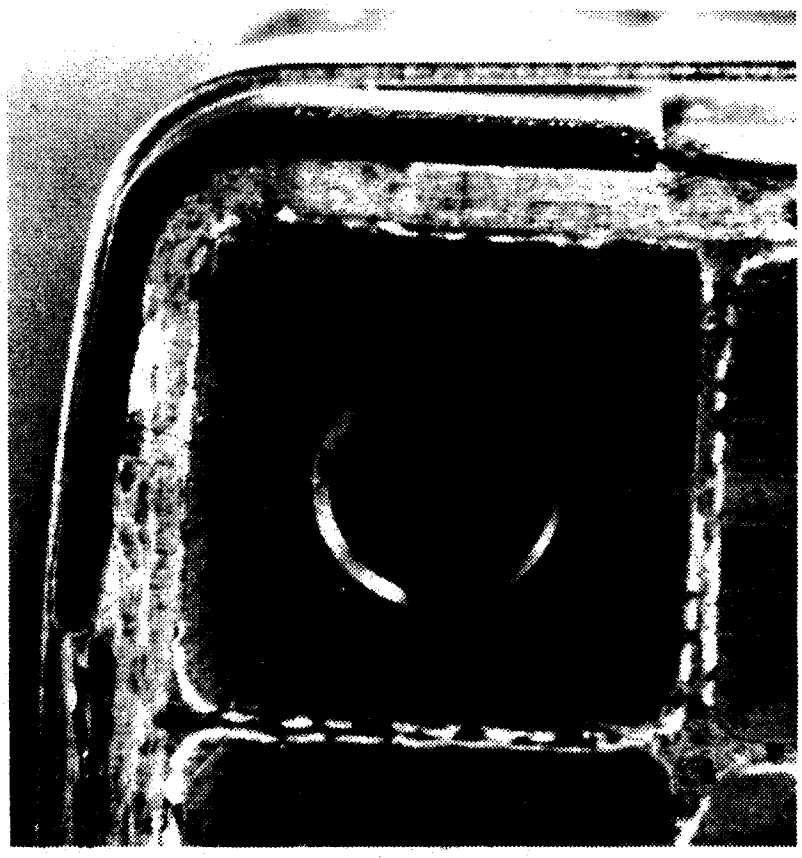

Fig. 22 Detail of bending magnet coil showing corner conductor and ground insulation

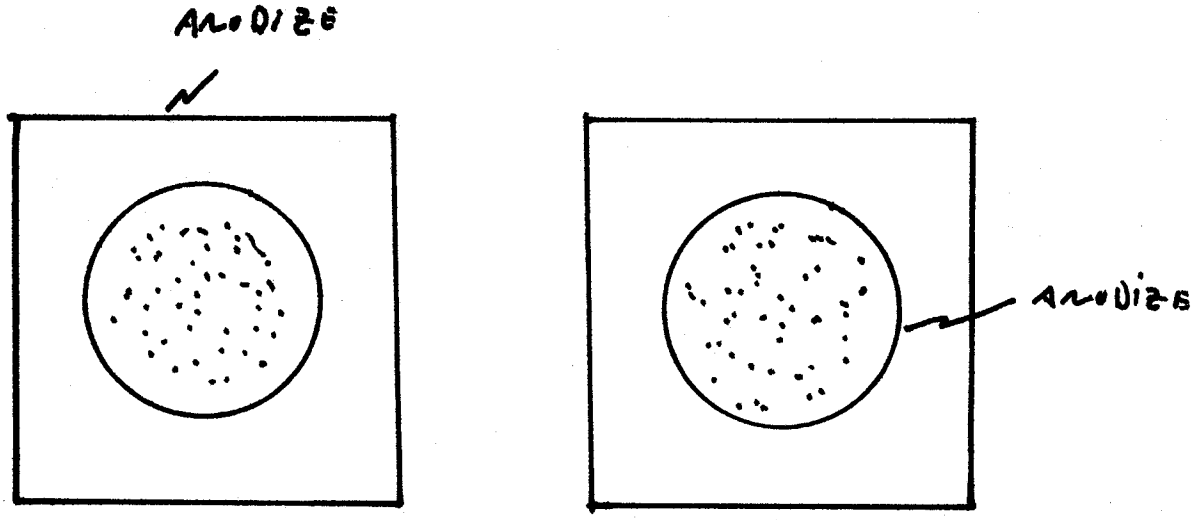

ALUMINUM
CONDUIT

SUPERCONDUCTING
VERSION

Time-of-flight, Bonner Spheres and ^{3}He detectors require low intensity

Need different measurements/geometries:

- High energy spectra at high intensities
- All neutron spectra at low intensity
- All neutrons and angular distribution at low intensity
- All neutrons in simulated target geometry at high intensity
- All neutrons in simulated target geometry (including backscatter) at low intensity

Need benchmaking to give accurate results.

A factor of 2 makes a very large difference in how you might build the magnets.